Modifying the refined zigzag theory to incorporate functional gradation into the bending analysis of laminated beams

Joseph R. S. Rodrigues[1], Fabio C. da Rocha[1], Maria do S. M. Sampaio[2], Leslie D. P. Fernández[3], Julián B. Castillero[4]

[1]*Dept. of Civil Engineering (DEC/UFS), Postgraduate Program in Civil Engineering (PROEC/UFS)*
Av. Marcelo Deda Chagas, 49107-230, São Cristóvão - SE, Brazil
richard_rck@academico.ufs.br, fabiocrocha@academico.ufs.br
[2]*Dept. of Civil Engineering, University of Amazonas State*
Darcy Vargas Avenue, 69050-020, Amazonas/Manaus, Brazil
msampaio@uea.edu.br
[3]*Dept. of Mathematics and Statistic, Federal University of Pelotas*
Campus Universitário, Capão do Leão, 96160-000, Pelotas - RS, Brazil
leslie.fernandez@ufpel.edu.br
[4]*IIMAS Academic Unit at Yucatán, National Autonomous University of Mexico*
Car. Mérida-Tetiz km 4.5, 97357, Ucú - Yu, Mexico
julian@mym.iimas.unam.mx

Abstract. Extensive research has been conducted in the field of composite materials, particularly in laminated composites. However, laminated composites often face challenges such as stress concentration at interfaces due to the sharp differences in properties between layers. This study proposes an approach to mitigate stress concentrations in laminated beams using functionally graded materials (FGMs). Functional gradation is achieved by continuously varying properties across the thickness of each beam layer. The modeling is based on the refined zigzag theory (RZT), with an additional introduction of the sublayers to capture the functional gradation. The analysis involves deriving the zigzag function for FGM, which is referred to as modified RZT. Subsequently, the kinematic model is applied based on the principle of minimum total energy to derive the Euler equation and its associated boundary conditions. For analytical resolution, the Navier procedure is employed. The results obtained for displacement and tension fields are compared with other formulations from the literature, which exhibit good agreement and therefore validate the proposed method.

Keywords: laminated beams, functionally graded materials, modified refined zigzag theory.

1 Introduction

The demand for solutions that meet high-performance requirements in civil, mechanical, and aerospace engineering has driven the study of composite materials. According to Kaw [1], a composite is defined as a material composed of two or more constituents that are not soluble in each other and are combined at the macroscopic level. Combining materials to obtain a material with improved physical and chemical properties is a timeless practice. As Vinson and Sierakowski [2] report, ancient Israeli workers incorporated chopped straw into bricks to enhance their structural performance.

Among the various types of composites, laminates are particularly notable for their widespread applications in structures such as beams and plates. Laminates are characterized by the strategic stacking of layers of different materials to create structures with high mechanical performance. However, as Thai and Vo [3] have noted, laminated composites under load are susceptible to stress concentrations at the interfaces between layers. This issue can be mitigated by incorporating functionally graded materials (FGMs) into the structure, as Sayyad and Ghugal [4] suggest. FGMs are distinguished by a continuous variation of material properties from one interface to another, which helps to alleviate stress concentrations. According to Pu et al. [5], this gradual change in properties across the material enhances the structural performance and durability of FGMs.

Due to the high heterogeneity of the cross-sections of laminated composites, Tessler et al. [6] proposed a high-order beam theory capable of accurately modeling their displacement and stress fields, calling it the refined zigzag theory (RZT). However, the original RZT only considers constant material properties. Therefore, this work aims to develop a modified RZT formulation by incorporating FGMs into its theoretical framework for the static analysis of laminated composite beams subjected to bending. The functional gradation is integrated into our formulation using the fictitious sublayer technique presented by Chen and Su [7]. Euler equations and their respective boundary conditions are derived from the principle of minimum total energy. We solve the problem analytically using the Navier procedure and analyze the response fields by varying parameters such as grading index, layer thickness, and the length-to-total thickness ratio of the beam.

2 Methodology

Consider a supported FGM beam subjected to a load $q(x)$, referenced by the x and z axes, as shown in Fig. 1.

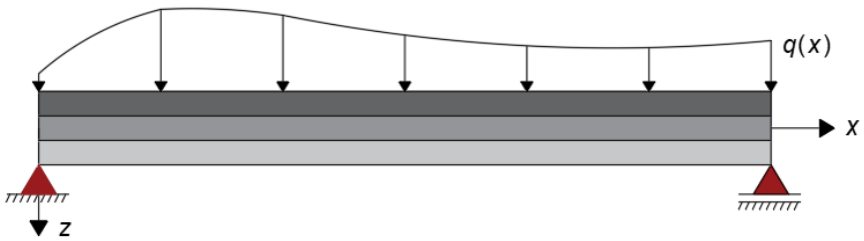

Figure 1. Transversely loaded FGM beam.

The displacement field is expressed as

$$u_x^{(k,n)}(x,z) = u_0(x) + z\theta(x) + \phi^{(k,n)}(x,z)\psi(x),\ k = 1, 2, ..., \overline{N},\ n = 1, 2, ..., N, \tag{1}$$

$$u_z(x,z) = w(x), \tag{2}$$

where u_x and u_z denote the axial and transverse displacements, respectively. k and n represent the kth and nth layers and sublayers, respectively. Additionally, $\overline{N}$ and N represent the last layer and last sublayer, respectively. The axial displacement in the midplane of the beam is denoted by u_0, the rotation of the cross-section by θ, the zigzag function by ϕ, the amplitude of the zigzag function by ψ, and the deflection by w, respectively.

The zigzag function is expressed by

$$\phi^{(k,n)}(x,z) = \left(\frac{z^{(k,n)} - z}{h^{(k)}/N}\right) u_x^{(k,n-1)}(x, z^{(k,n)}) + \left(\frac{z - z^{(k,n-1)}}{h^{(k)}/N}\right) u_x^{(k,n)}(x, z^{(k,n)}), \tag{3}$$

where the thickness of each layer is denoted by $h^{(k)}$ and the total thickness of the beam is denoted by h. The term $z^{(k,n)}$ represents the thickness coordinate at the interface between the $(n-1)$th and the nth sublayer of the kth layer, expressed as

$$z^{(k,n)} = z^{(k-1)} + \frac{n}{N} h^{(k)}. \tag{4}$$

The slope of the zigzag function is defined by

$$\beta^{(k,n)}(x) = \phi_{,z}^{(k,n)}. \tag{5}$$

where the subscripted comma notation indicates differentiation with respect to the variable(s) to its right. By differentiating eq. (3) with respect to z and substituting it into eq. (5), we obtain

$$\beta^{(k,n)}(x) = \frac{u_x^{(k,n)} - u_x^{(k,n-1)}}{h^{(k)}/N}. \tag{6}$$

The strain field is obtained by differentiating eq. (1) and eq. (2) as

$$\varepsilon_x^{(k,n)}(x,z) = u_{x,x}^{(k,n)} = u_{0,x} + z\theta_{,x} + \phi^{(k,n)}\psi_{,x}, \tag{7}$$

$$\gamma_{xz}^{(k,n)}(x,z) = u_{x,z}^{(k,n)} + u_{z,x} = w_{,x} + \theta + \beta^{(k,n)}\psi, \tag{8}$$

where ε_x and γ_{xz} represent the axial and shear strains, respectively. From eq. (7) and eq. (8), the corresponding stress field can be obtained as

$$\sigma_x^{(k,n)}(x,z) = E_x^{(k,n)}\varepsilon_x^{(k,n)} = E_x^{(k,n)}\left(u_{0,x} + z\theta_{,x} + \phi^{(k,n)}\psi_{,x}\right), \tag{9}$$

$$\tau_{xz}^{(k,n)}(x,z) = G_{xz}^{(k,n)}\gamma_{xz}^{(k,n)} = G_{xz}^{(k,n)}\left(w_{,x} + \theta + \beta^{(k,n)}\psi\right), \tag{10}$$

where σ_x and τ_{xz} denote the axial and shear stresses, respectively. E and G represent the longitudinal and shear moduli of elasticity, respectively. For algebraic manipulation of eq. (10), we introduce

$$\gamma = w_{,x} + \theta, \tag{11}$$

$$\eta = \gamma - \psi, \tag{12}$$

where γ denotes the average shear strain and η denotes the auxiliary function. Substituting eq. (11) and eq. (12) into eq. (10), the shear stress can be rewritten as

$$\tau_{xz}^{(k,n)}(x,z) = G_{xz}^{(k,n)}\eta + G_{xz}^{(k,n)}\left(1 + \beta^{(k,n)}\right)\psi. \tag{13}$$

The RZT enforces the continuity of shear stress between layers. Thus, the second term of eq. (13) is defined as constant, that is,

$$G = G_{xz}^{(k,n)}\left(1 + \beta^{(k,n)}\right), \tag{14}$$

where G represents the average shear modulus. Isolating $\beta^{(k,n)}$ we find

$$\beta^{(k,n)} = \frac{G}{G^{(k,n)}} - 1. \tag{15}$$

However, based on the RZT assumption that $u^{(1,0)} = 0$ and $u^{(\overline{N},N)} = 0$, it is verified that the integration of the slope of the zigzag function over the cross-sectional area of the beam yields zero, that is,

$$\int_A \beta^{(k,n)} dA = 0. \tag{16}$$

where A denotes the cross-sectional area of the beam. Integrating eq. (15) over the cross-sectional area and applying the property stated in eq. (16), the average shear modulus can be expressed as

$$G = \frac{h}{\sum_{k=1}^{\overline{N}} \sum_{n=1}^{N} \frac{h^{(k)}}{NG^{(k,n)}}}. \tag{17}$$

The axial displacements at the interfaces can be expressed in terms of the shear moduli by substituting eq. (15) into eq. (6), that is,

$$u_x^{(k,n)}(x,z) = u_x^{(k,n-1)} + \left(\frac{G}{G^{(k,n)}} - 1 \right) \frac{h^{(k)}}{N}. \tag{18}$$

Substituting eq. (17) into eq. (18), we obtain the recurrence formula given by

$$u_x^{(k,n)}(x,z) = u_x^{(k,n-1)} + \frac{h^{(k)}}{N} \left[\frac{h}{G^{(k,n)} \sum_{m=1}^{\overline{N}} \sum_{r=1}^{N} \frac{h^{(m)}}{NG^{(m,r)}}} - 1 \right]. \tag{19}$$

Verifying the recurrence formula presented in eq. (19) for each sublayer, it is observed that the axial displacements can be expressed independently of the previous sublayer as

$$u_x^{(k,n)}(x,z) = \frac{h}{\sum_{m=1}^{\overline{N}} \sum_{r=1}^{N} \frac{h^{(m)}}{NG^{(m,r)}}} \left[\sum_{m=1}^{k-1} \sum_{r=1}^{N} \frac{h^{(m)}}{G^{(m,r)}N} + \sum_{r=1}^{n} \frac{h^{(k)}}{G^{(k,r)}N} \right] - \left(\frac{h}{2} + z^{(k,n)} \right). \tag{20}$$

It is defined that the zigzag function takes the same value as the axial displacements at the interfaces, that is,

$$\phi^{(k,n)}(x,z)|_{z=z^{(k,n)}} = u_x^{(k,n)}(x,z). \tag{21}$$

Substituting eq. (20) into eq. (21) and taking the limit as N tends to infinity yields

$$\widehat{\phi}^{(k)}(x,z) = \lim_{N \to \infty} u_x^{(k,n)} = \frac{h \sum_{m=1}^{k-1} \int_{z^{(m-1)}}^{z^{(m)}} \frac{dz}{G^{(m)}} + \int_{z^{(k-1)}}^{z} \frac{dz}{G^{(k)}}}{\sum_{m=1}^{\overline{N}} \int_{z^{(m-1)}}^{z^{(m)}} \frac{1}{G^{(m)}} dz} - \left(z + \frac{h}{2} \right), \tag{22}$$

where $\widehat{\phi}^{(k)}$ denotes the modified zigzag function whose slope is given by $\widehat{\beta}^{(k)} = \widehat{\phi}^{(k)}_{,z}$. From these functions, the response fields are now expressed as

$$u_x^{(k)}(x,z) = u_0(x) + z\theta(x) + \widehat{\phi}^{(k)}(x,z)\psi(x), \tag{23}$$

$$u_z = w(x), \tag{24}$$

$$\varepsilon_x^{(k)}(x,z) = u_{x,x}^{(k)} = u_{0,x}(x) + z\theta_{,x}(x) + \widehat{\phi}^{(k)}(x,z)\psi_{,x}(x), \tag{25}$$

$$\gamma_{xz}^{(k)}(x,z) = u_{x,z}^{(k)} + u_{z,x} = w_{,x}(x) + \theta(x) + \widehat{\beta}^{(k)}(x)\psi(x), \tag{26}$$

$$\sigma_x^{(k)}(x,z) = E^{(k)}(z)\varepsilon_x^{(k)}(x,z), \tag{27}$$

$$\tau_{xz}^{(k)}(x,z) = G^{(k)}(z)\gamma_{xz}^{(k)}(x,z). \tag{28}$$

3 Main results

The results for the displacement and stress fields were obtained analytically for a simply supported FGM beam subjected to a uniformly distributed load, where the effective moduli of elasticity are defined by

$$E^{(k)}(z) = E_b^{(k)} + \left(E_t^{(k)} - E_b^{(k)}\right)\left(\frac{z - z^{(k-1)}}{z^{(k)} - z^{(k-1)}}\right)^{\alpha^{(k)}},\ z \leq 0, \tag{29}$$

$$E^{(k)}(z) = E_t^{(k)} + \left(E_b^{(k)} - E_t^{(k)}\right)\left(\frac{z^{(k)} - z}{z^{(k)} - z^{(k-1)}}\right)^{\alpha^{(k)}},\ z > 0, \tag{30}$$

$$G^{(k)}(z) = \frac{E^{(k)}}{2\left(1 + \nu^{(k)}\right)}, \tag{31}$$

where $E_b^{(k)}$ and $E_t^{(k)}$ denote the longitudinal moduli of elasticity at the bottom and the top of the kth layer, respectively. The gradation index in the kth layer is represented by $\alpha^{(k)}$. The Poisson ratio in the kth layer is denoted by $\nu^{(k)}$.

The laminate is composed of metal and ceramic, as shown in Table 1. The metal is arranged in the face layers, while the ceramic forms the intermediate layer of the laminate, representing the rigid core of the structure.

Table 1. Composition of the FGM laminate

Layer	Material	$E^{(k)}$ (GPa)	$\nu^{(k)}$
1	Metal	70	0,30
2	Ceramic	323	0,30
3	Metal	70	0,30

Regarding the geometric properties of the beam, it has a length-to-thickness ratio $L/h = 10$. The results were produced for various layer thickness ratios, as detailed in Table 2.

Table 2. Layer thickness ratio

Thickness ratio	Layer 1	Layer 2	Layer 3
1-2-1	$h/4$	$h/2$	$h/4$
1-1-1	$h/3$	$h/3$	$h/3$
2-1-1	$h/2$	$h/4$	$h/4$
2-2-1	$2h/5$	$2h/5$	$h/5$

The results obtained were validated against the work by Vinh [8], which addresses the theory of first-order shear deformation and solves the problem numerically. The dimensionless parameters of thickness coordinate, deflection, and stress are

$$\widetilde{z} = \frac{z}{h},\ \widetilde{w}(x) = \frac{10E_c h_0^3}{q_0 L^4} w(x),\ \widetilde{\sigma}_x^{(k)}(L/2\,, \widetilde{z}) = \frac{h_0}{q_0 L}\sigma_x^{(k)}(L/2\,, \widetilde{z}), \tag{32}$$

where $q(x) = q_0$ as it is a uniformly distributed load, E_c represents the longitudinal modulus of elasticity of the ceramic and $h_0 = L/10$.

Figure 2a illustrates the variation of the effective longitudinal modulus across the thickness for a 1-2-1 laminate considering various grading indices. It is observed that for a grading index of zero, the effective modulus corresponds to the core value, i.e., the ceramic. For grading indices greater than zero, the effective modulus transitions from the modulus of the metal to that of the ceramic. Depending on how high the grading index is, the ceramic modulus tends to be reached very quickly as the thickness coordinate approaches the metal-ceramic interface.

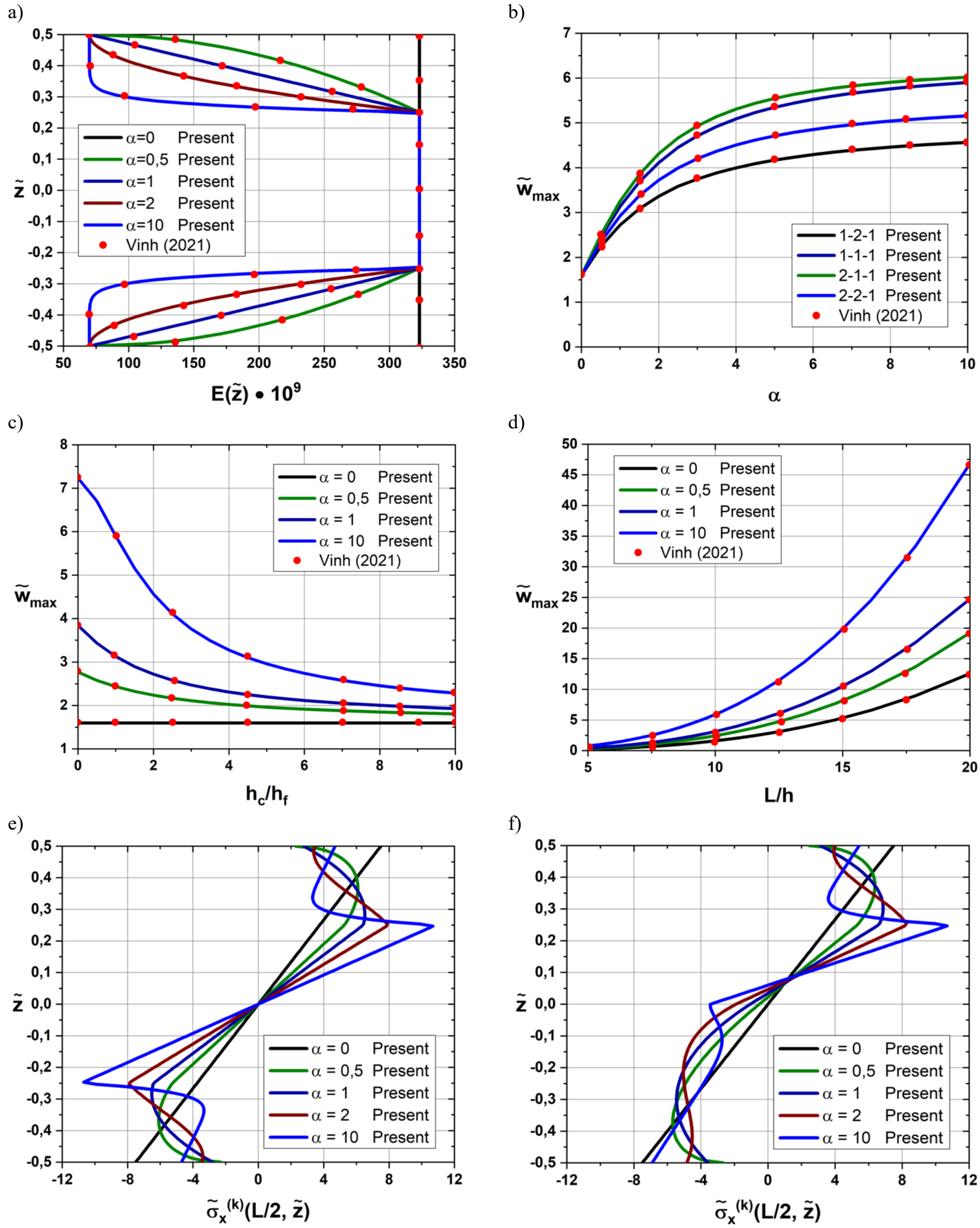

Figure 2. a) variation of the effective modulus across the thickness for a 1-2-1 laminate, b) maximum normalized deflection versus grading index for different thickness ratios, c) maximum normalized deflection versus thickness ratio between core and face, d) maximum normalized deflection versus length-to-total thickness ratio of the beam for a 1-1-1 laminate, e) distribution of normalized axial stresses along the thickness for a 1-2-1 laminate, f) distribution of normalized axial stresses along the thickness for a 2-1-1 laminate

Figure 2b illustrates the relationship between maximum deflection and graded-index for various thickness ratios. The curves exhibit higher slopes at lower graded-index values, with decreasing growth rates as the index increases. The laminate with a 2-1-1 ratio shows the highest maximum deflection values.

Figure 2c depicts the maximum deflection versus the thickness ratio between the core and face of the laminate for different graded indexes. At an index of zero, the maximum deflection remains constant regardless of h_c/h_f. For indexes greater than zero, increasing h_c/h_f results in decreased maximum deflection values due to increased structural stiffness. Notably, the highest maximum deflection values are observed at $h_c/h_f = 0$, indicating the absence of a rigid core.

Figure 2d illustrates the maximum deflection versus the length-to-total thickness ratio of the beam for a 1-1-1 laminate. At $L/h = 5$, the maximum deflection values are nearly identical across all curves. As the ratio L/h increases, the maximum deflection in the beam also increases, indicating greater deflection as the beam becomes more slender. Moreover, higher grading indices correspond to higher maximum deflection values

Figure 2e displays the distribution of normalized axial stress along the thickness for a symmetric 1-2-1 laminate, whereas Fig. 2f illustrates an asymmetric 2-1-1 laminate. In both cases, the stress distribution is linear across the thickness when the grading index is zero. With higher grading indices, the stress profile becomes nonlinear in the face layers while remaining linear in the core layer. Increasing the graded-index accentuates axial stresses at the interfaces yet maintains continuity.

4 Conclusions

This study modified the RZT formulation to incorporate functional gradation using the fictitious sublayer technique, applied to functionally graded laminated composite beams subjected to bending. The analysis comprehensively examined displacement and stress fields, varying parameters such as gradation index, layer thickness, and beam length-to-total thickness ratio. Higher-graded index values and varying layer proportions were found to intensify axial stresses at interfaces. The results showed strong agreement with existing literature, confirming the effectiveness of the proposed RZT modification for static beam analysis.

Acknowledgements. The authors thank CNPq for financial support (Universal Project No. 402857/2021-6). FCR, LSPF, and JBS also thank FAPITEC (Universal Project No. 019203.01702/2024-6), with FCR extending thanks to the FAPITEC/SE/FUNTEC Call No. 02/2024.

Authorship statement. The authors hereby confirm that they are the sole liable persons responsible for the authorship of this work, and that all material that has been herein included as part of the present paper is either the property (and authorship) of the authors, or has the permission of the owners to be included here.

References

[1] A. K. Kaw. *Mechanics of Composite Materials*. CRC Press, 2005.

[2] J. R. Vinson and R. L. Sierakowski. *The Behavior of Structures Composed of Composite Materials*. Springer, 2008.

[3] H.-T. Thai and T. P. Vo. Bending and free vibration of functionally graded beams using various higher-order shear deformation beam theories. *International Journal of Mechanical Sciences*, vol. 62, pp. 57–66, 2012.

[4] A. S. Sayyad and Y. M. Ghugal. Modeling and analysis of functionally graded sandwich beams: a review. *Mechanics of Advanced Materials and Structures*, vol. 26, n. 21, pp. 1776–1795, 2018.

[5] Y. Pu, S. Jia, Y. Luo, and S. Shi. Bending analysis of functionally graded sandwich beams with general boundary conditions using a modified fourier series method. *Archive of Applied Mechanics*, vol. 93, pp. 3741–3760, 2023.

[6] A. Tessler, M. D. Sciuva, and M. Gherlone. A refined zigzag beam theory for composite and sandwich beams. *Journal of Composite Materials*, vol. 43, pp. 1051–1081, 2009.

[7] C.-D. Chen and P.-W. Su. An analytical solution for vibration in a functionally graded sandwich beam by using the refined zigzag theory. *Acta Mechanica*, vol. 232, pp. 4645–4668, 2021.

[8] P. V. Vinh. Static bending analysis of functionally graded sandwich beams using a novel mixed beam element based on first-order shear deformation theory. *Forces in Mechanics*, vol. 4, pp. 100039, 2021.